Science of the Total Environment 797 (2021) 149103

Contents lists available at ScienceDirect

Science of the Total Environment

journal homepage: www.elsevier.com/locate/scitotenv

Uranium isotopes as a possible tracer of terrestrial authigenic carbonate

Leja Rovan [a,b], Tea Zuliani [a,b], Barbara Horvat [c], Tjaša Kanduč [a], Polona Vreča [a], Qasim Jamil [b], Branko Čermelj [d], Elvira Bura-Nakić [e], Neven Cukrov [e], Marko Štrok [a,b,*], Sonja Lojen [a,f]

[a] Department of Environmental Sciences, Jožef Stefan Institute, Jamova cesta 39, 1000 Ljubljana, Slovenia
[b] Jožef Stefan International Postgraduate School, Jamova cesta 39, 1000 Ljubljana, Slovenia
[c] Slovenian National Building and Civil Engineering Institute, Dimičeva ulica 12, 1000 Ljubljana, Slovenia
[d] Marine Biology Station, National Institute of Biology, Fornače 40, 6330 Piran, Slovenia
[e] Division for Marine and Environmental Research, Ruđer Bošković Institute, Bijenička cesta 54, 10000 Zagreb, Croatia
[f] School of Environmental Sciences, University of Nova Gorica, Glavni trg 8, 5271 Vipava, Slovenia

HIGHLIGHTS

- New insight of understanding possible environmental influences on tufa formation
- Combination use of traditional and U isotopes was evaluated in the karst aquifer.
- U isotopic composition was analysed with MC-ICP-MS.
- $\delta^{13}C$, $\delta^{18}O$ and U values confirmed carbonates authigenic origin.
- U isotopes are relevant for the construction of the CO_2 mass balance.

GRAPHICAL ABSTRACT

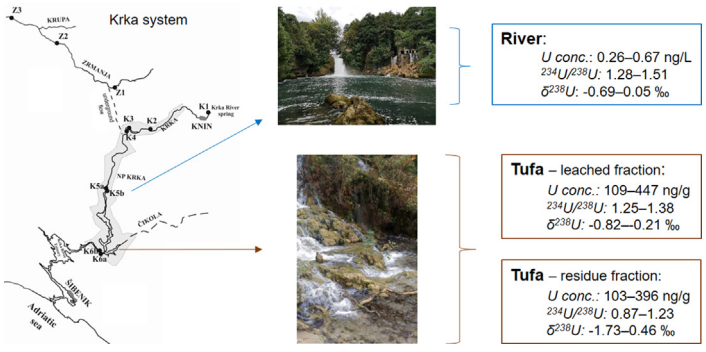

ARTICLE INFO

Article history:
Received 6 May 2021
Received in revised form 13 July 2021
Accepted 13 July 2021
Available online 17 July 2021

Editor: Filip M.G. Tack

Keywords:
Uranium isotopes
Karst aquifer
Authigenic carbonate
Tufa
Krka River

ABSTRACT

The concentration and isotopic composition of uranium ($\delta^{238}U$, $^{234}U/^{238}U$ activity ratio) in combination with traditional isotopes ($\delta^{18}O$, $\delta^{13}C$) were examined as potential tracers of authigenic carbonate formation in a karst aquifer. The U concentration and $^{234}U/^{238}U$ activity ratios in the tufa-precipitating sections of two connected karst rivers (Krka and Zrmanja, Croatia) decreased downstream in water and in precipitated carbonate due to active self-purification processes, i.e. adsorption of isotopically lighter U(VI) on mineral particles, sedimentation and co-precipitation with carbonate. The isotopic composition of carbonate in tufa mostly resembled the $^{234}U/^{238}U$ activity ratio and the $\delta^{238}U$ values of dissolved U in water but was also affected by the presence of detrital carbonate flushed into the river from soil and weathered bedrock. This interpretation was supported by the $\delta^{18}O$ and $\delta^{13}C$ values of tufa, which were shifted out of equilibrium with river water and dissolved in organic carbon and in their isotopic signature, which showed the presence of lithic carbonate. Large fluctuations of the $\delta^{238}U$ values of water, leachable U (eluted in acetic acid buffered with Na-acetate) and residual U fraction could not be fully explained by available data due to the overlapping U isotopic signatures of leachable (mainly carbonate) and residual fractions of soil, bedrock and tufa. Therefore, a long-term, systematic, seasonal and event-based observation of the isotopic composition of dissolved and suspended particulate U in water is necessary. Nevertheless, the U isotopes were found to have the potential to be used as identifiers of authigenic carbonate and the storage of CO_2 in terrestrial river sediments, to improve knowledge on fluxes within local and global biogeochemical carbon cycle.

* Corresponding author at: Department of Environmental Sciences, Jožef Stefan Institute, Jamova cesta 39, 1000 Ljubljana, Slovenia.
E-mail address: marko.strok@ijs.si (M. Štrok).

https://doi.org/10.1016/j.scitotenv.2021.149103

1. Introduction

The formation of authigenic carbonate has only recently been invoked as the third major global carbon sink (Zhao et al., 2016). Therefore, the identification of authigenic carbonate in marine and terrestrial settings is crucial for the estimation of the magnitude and locations of carbon fixation. The identification of authigenic terrestrial carbonates is usually based on their carbon and oxygen isotopic compositions (Leng et al., 2006). The terrestrial dissolved inorganic carbon (DIC) is usually depleted in ^{13}C compared to marine DIC, and the water from which the terrestrial carbonates are precipitated is usually significantly depleted in ^{18}O compared to the seawater (Gat and Gonfiantini, 1981). In principle, both C ($\delta^{13}C$) and O ($\delta^{18}O$) isotopic compositions should be conspicuous enough to be used as identifiers of authigenic carbonate. However, in terrestrial environments, multiple sources of DIC with different or overlapping isotopic compositions do not allow for such appointment of a carbonate formation pathway. Spatially and temporally variable precipitation rates, cyclic episodes of deposition and erosion, mixing with detrital minerals, disequilibrium effects and diagenetic processes can affect the δ values of bulk terrestrial carbonate (Brasier et al., 2010; De Boever et al., 2017; Zavadlav et al., 2017; Yan et al., 2020), which can make the source appointment of carbonate uncertain.

Zhao et al. (2016) identified U concentrations in a cross-plot with the C isotope composition as the potential identifier of authigenic carbonate in limestone. The isotopes of U have already been proven in karst hydrogeology to be a useful tool for identifying young carbonates (Bourdon et al., 2009; Nyachoti et al., 2019), but a systematic analysis of U isotope fractionation in carbon cycle of a river has not been explored yet. In karst aquifers, U is released into the groundwater from bedrock and soil during weathering. Young karst groundwater is characterised by a dissolved $^{234}U/^{238}U$ activity ratio higher than the secular equilibrium of the U-series isotopes that is found in bedrock due to the so-called alpha recoil effect (Chen et al., 2020; Fleischer, 1982; Suksi et al., 2006). Therefore, the dissolved $^{234}U/^{238}U$ activity ratios are often used in hydrology as a tracer for studying spatial changes in bedrock lithology and the mixing of water from different sources (Chabaux et al., 2003; Chabaux et al., 2008; Bourdon et al., 2009). During precipitation, the dissolved $^{234}U/^{238}U$ activity ratio of water is transferred to the carbonate without any apparent fractionation. The authigenic carbonate should thus be distinguished from the marine carbonate formed in geological history by its elevated $^{234}U/^{238}U$ activity ratio (Teichert et al., 2003; Bourdon et al., 2009; Andersen et al., 2010; Wang and You, 2013; Andersen et al., 2017).

Natural variations in $^{238}U/^{235}U$, usually reported as $\delta^{238}U$ values, are in the permil range and can be primarily associated with the variable solubility of U in different redox states, adsorption or leaching, mostly due to thermodynamic or nuclear field shift effects (Stirling et al., 2007; Weyer et al., 2008; Brennecka et al., 2011). The co-precipitation of U in calcite from an aquatic solution is not associated with isotope fractionation. Therefore, similar to $^{234}U/^{238}U$ activity ratio, the $\delta^{238}U$ values of carbonate resemble those of the precipitating water (Chen et al., 2016) and depend mostly on the redox conditions in the basin (Andersen et al., 2017, and references therein).

Tufa is a terrestrial sediment most commonly composed of authigenic calcium carbonate precipitated at an ambient temperature from supersaturated water in rivers, springs or lakes (Ford and Pedley, 1996; Pedley, 2009) and represents an ideal material for investigation and testing of potential identifiers of terrestrial authigenic carbonate. It can contain variable amounts of mineral and organic detritus contributed by the surface runoff from soil and bedrock erosion or from autochthonous particulate organic matter. The precipitation of $CaCO_3$ in a supersaturated river follows the degassing of dissolved CO_2 at springs and at or close to the topographic discontinuities (e.g. rapids, waterfalls) along the watercourse. It is usually facilitated (or even induced) by the presence of biofilms and macrobiota, which influence the chemical and isotopic characteristics of precipitates (Rogerson et al., 2008; Banks and Jones, 2012; Capezzuoli et al., 2014; Saunders et al., 2014). Tufa formation is thus an important process of the continental CO_2 cycle that accounts for the evasion of CO_2 from the river to the atmosphere as well as for the fixation of CO_2 in a carbonate sediment. Tufa as a CO_2 sink may indeed be rather small on a global scale, but it can play a considerable role in karst landscapes (González Martín and González Amuchastegui, 2014).

The aim of this study was to test the U isotopes as a potential identifier of authigenic carbonate in a specific terrestrial depositional setting of two hydraulically connected karst rivers (Krka and Zrmanja, Croatia). The spatial variability of geochemical (U/Ca) and isotopic ($\delta^{18}O$, $\delta^{13}C$, $\delta^{238}U$, and $^{234}U/^{238}U$ activity ratio) parameters were investigated in river water, in a series of tufa cascades and in the soil and bedrock, which are the two main sources of dissolved and detrital materials for tufa precipitation. The U isotope fractionation between river water and carbonate in tufa was estimated to provide complementary information to traditional (O, C) isotopes needed to differentiate between authigenic and detrital carbonate in tufa and to quantify the authigenic carbonate formation in karst rivers.

2. Study area

Krka River is a 75 km long karstic stream in Central Dalmatia, Croatia (Fig. 1), with an estimated drainage area of 2427 km^2 (Bonacci et al., 2006). The entire catchment is located at the Outer Dinaric carbonate platform composed mainly of Cretaceous limestone with some sporadic dolomite and Eocene limestone interchanged with clastic rocks (marl, conglomerate and flysch) (Mamudžic, 1971). In the wider area of Knin ~3 km downstream from the spring, small outcrops of the so-called Dinaride evaporitic mélange occur, which are composed of Permian to Triassic evaporites (gypsum, anhydrite and some sporadic dolomite) and associated sedimentary and igneous blocks, sometimes embedded within evaporites (Kulušic and Borojevic Šostaric, 2014; Dedic et al., 2018). Two intermittent streams, Orašnica and Butišnica, drain these formations and discharge their weathering products into the Krka River near Knin.

The river is mainly groundwater-fed with some minor intermittent tributaries. The discharge at the spring varies between 1.5 and 10 $m^3\ s^{-1}$, while the discharge at the Skradinski buk waterfall at the head of the estuary is on average 51.3 $m^3\ s^{-1}$ (ranging from 5 to 476 $m^3\ s^{-1}$) (Bonacci et al., 2017). Previous studies have shown that a massive diffuse subsurface recharge from the northeast from the Zrmanja River takes place in the flow section between 18.8 and 22 km downstream from the spring, which contributes a considerable fraction of the water flow to the lower reaches of the stream (Bonacci, 1999; Lojen et al., 2004; Bonacci et al., 2006).

At present, tufa occurs along 50 km of the watercourse with a total fall of 242 m. The river is sectioned by nine larger barriers and numerous smaller cascades into a series of lentic and lotic environments (Cukrov et al., 2013). The recent measurements revealed highly variable annual tufa growth rates between <1 mm and 2 cm (Maric et al., 2020).

3. Materials and methods

3.1. Sampling

Samples of water, tufa, bedrock and soil were collected in September 2019 at the main cascades at Krka River (samples K1 to K6) and at Zrmanja River (samples Z1 to Z3, Fig. 1). The seasonal sink of the Zrmanja River occurs between sites Z1 and Z2.

The water samples for the analyses of the total alkalinity and isotope composition of DIC were filtered on-site through 0.2 μm pore-sized membrane filters (Sartorius Minisart 16534K) and stored in 100 mL high-density polyethylene (HDPE) bottles (for alkalinity) and 12 mL glass vials with septum caps without headspace (Labco Exetainer® for

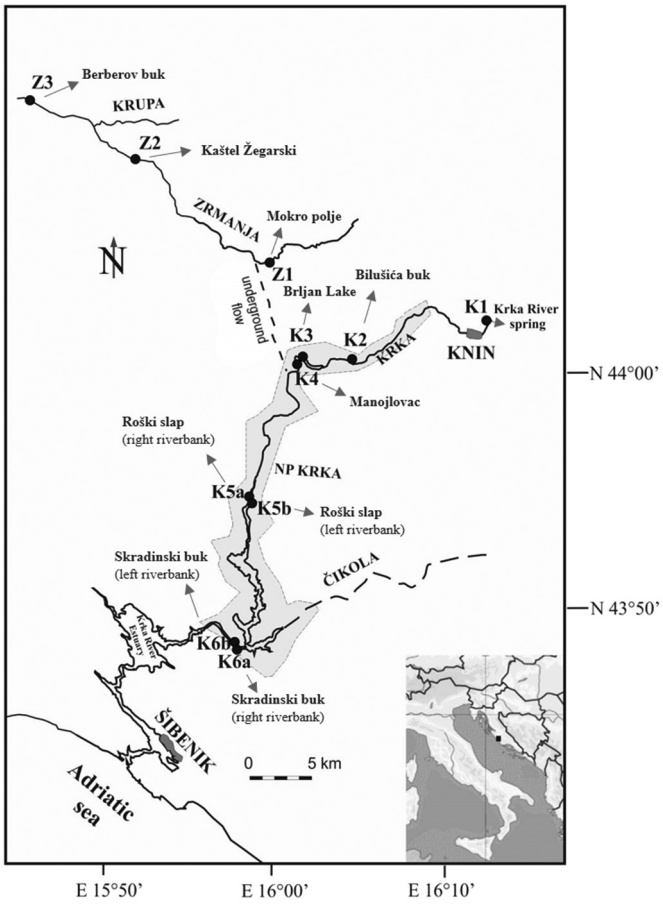

Site; Sample material	Distance from the spring [km]	Altitude [m a.s.l.]	Type of tufa	Coordinates (Google Earth Pro)
K1; W, B, S	0	224		44°02'30" N 16°14'05.60" E
K2; W, T, B, S	16	208	cascade	44°00'47.39" N 16°04'06.35" E
K3; W, T, B, S	18.8	186	dam	44°00'33.63" N 16°02'37.04" E
K4; W, T, B, S	19.7	150	cascade	44°00'54.95" N 16°01'35.94" E
K5a; W, T, S **K5b**; W, T, B, S	35 35.5	72 70	paludal	43°54'30.02" N 15°58'39.20" E
K6a; W, T, S **K6b**; W, T	49 49.5	34 32	cascade	43°48'13.04" N 15°57'54.19" E
Z1; W, B	16	196		44°05'31.65" N 16°02'01.18" E
Z2; W	38	55		44°09'43.09" N 15°51'27.98"E
Z3; W, T, S	50	19	paludal	44°11'46.87" N 15°46'10.56" E

Fig. 1. Site map and sampling sites in the Krka-Zrmanja river system with a response legend of sampling locations and sampled material at Krka River (K) and Zrmanja River (Z); W = water, B = bedrock, S = soil, T = tufa.

δ^{13}C-DIC analysis). Samples for the water isotope analyses were kept unfiltered in 30 mL HDPE bottles without headspace. Samples for the major metal analyses were filtered through 0.45 μm pore-sized membrane filters (Sartorius Minisart 16555K) into pre-washed HDPE bottles and acidified on-site with supra pure HNO_3 (65%, Merck) to pH ≤ 1.5. All samples were kept refrigerated at 4–8 °C until analysis. For the analysis of U isotopes, 1 L samples were kept in prewashed PE bottles in a cool box and transported to the laboratory, where they were vacuum filtered through a 0.45-μm pore-sized Millipore membrane filter. After filtration, the samples were acidified with concentrated supra-pure HNO_3.

Three to five hand samples of recent tufa were collected from the riverbed at each site. Soil and rock samples were collected at outcrops adjacent to the tufa sampling sites.

3.2. Analyses

3.2.1. River water

Water temperature, pH, electrical conductivity and redox potential (Eh) were measured on-site with the multiprobe Ultrameter II 6 PFC (Myron Company, Carlsbad, CA, USA). The total alkalinity was determined by Gran titration (Gieskes, 1974) in approx. 50 mL samples using 0.05 M HCl with a precision of ±1% within 8 h after sample collection. Major element concentrations (Ca and Mg) were determined by an Agilent 7900x ICP-MS (Agilent Technologies, Tokyo, Japan).

The isotopic compositions of oxygen (δ^{18}O) in the water were determined according to the modified IAEA Technical procedure note no. 43 (Tanweer et al., 2009) using the CO_2-H_2O equilibration techniques (Epstein and Mayeda, 1953; Avak and Brand, 1995). Measurements were performed with a dual-inlet isotope ratio mass spectrometer Delta Plus (Finnigan MAT GmbH, Bremen, Germany) with a custom-built automated CO_2-H_2O equilibrator HDOeq 48 Equilibration Unit (M. Jaklitsch).

All measurements were performed together with laboratory reference materials (LRM) calibrated periodically against primary IAEA calibration standards to the VSMOW/SLAP scale. The defined isotope values and measurement uncertainty of LRMs used for the normalisation of data and independent quality control were calculated using the Kragten method (Carter and Barwick, 2011). The results were normalised to VSMOW/SLAP using the Laboratory Information Management System for Light Stable Isotopes (LIMS) programme and were expressed in the standard δ notation (in ‰):

$$\delta_{\text{sample}}\ [‰] = \left(R_{\text{sample}}/R_{\text{standard}} - 1\right) \times 1000 \quad (1)$$

where R_{sample} and R_{standard} represent heavy-to-light isotope ratios ($^{18}O/^{16}O$) in a sample and an international standard, respectively. For the normalisation of the results, two in-house working standards calibrated to the VSMOW/SLAP scale with defined δ^{18}O values and estimated measurement uncertainties +0.36 ± 0.04‰ and −19.73 ± 0.02‰ were used, respectively. As an independent quality control, the third laboratory working standard with $\delta^{18}O = -9.12 \pm 0.04$‰ and certified commercial reference materials USGS 45 and USGS 47 were used. The average sample repeatability was 0.03‰.

For the determination of the isotopic composition of DIC, a volume of 100–200 μL of phosphoric acid was added to a septum-sealed vial (volume of 3.7 mL) and was then purged with pure He (6.0). 1 mL of the sample was then injected, and the headspace CO_2 was analysed (Miyajima et al., 1995; Spötl, 2005). The $\delta^{13}C_{DIC}$ values were determined using the mass spectrometer IsoPrime 100 coupled with the MultiflowBio equilibration module (Elementar Analysensysteme GmbH, Langenselbold,

Germany). To control the extraction procedure, a standard solution of Na_2CO_3 with a known $\delta^{13}C_{DIC}$ value of -10.8 ± 0.2‰ was used. The average sample repeatability was 0.2‰.

The concentration of particulate matter was determined using aliquots of 1 L river water filtered through pre-weighted glass fibre filters (Whatman GF/F) and dried until reaching a constant weight at 60 °C.

For the determination of U isotopes, the procedure reported by Rovan and Štrok (2019) was used. U from the water sample was co-precipitated with $Ca_3(PO_4)_2$ and separated on the UTEVA column. U isotopes were eluted in a clean beaker with 15 mL of 1 M HCl. The eluate was evaporated to dryness, and the dry residue was digested three times with a mixture of HNO_3 and H_2O_2 before the measurements to destroy any possible organic residue that might co-elute from the resin.

The PHREEQC programme was used to calculate the concentration of dissolved inorganic carbon, the distribution of C species and the saturation indices of water with respect to calcite (SI_{calc}) (Parkhurst and Appelo, 1999).

The calcite precipitation rate (R) was calculated as described by Zavadlav et al. (2017) using the diffusion boundary layer (DBL) model by Buhmann and Dreybrodt (1985) as

$$R = \alpha \cdot \left(\left[Ca^{2+}\right] - \left[Ca^{2+}\right]_{eq} \right) \quad (2)$$

where α is the reaction constant, and $[Ca^{2+}]$ and $[Ca^{2+}]_{eq}$ are the concentrations of dissolved Ca^{2+} in the solution and in the equilibrium with calcite at ambient conditions determined in the field. The α values considered the temperature range measured in the Krka River (between 15 and 23.6 °C). The DBL thickness was considered to be 100 μm given that the turbulent conditions in the river prevail, and for the available water layer thickness, a value of 10 cm was taken at all sampling sites (Liu et al., 1995; Liu and Dreybrod, 1997).

3.2.2. Tufa, bedrock and soil

Samples of bedrock, soil and tufa were dried at 105 °C until reaching a constant weight and were crushed in bras mortar. After the removal of all visible plant remains, the samples were pulverised in a vibrating disk mill (Siebtechnik GmbH, Germany) and sieved below 90 μm.

For the elemental analysis, disks melted in the furnace (Claisse, Malvern Panalanalytical, Malvern, U.K.) were prepared with a mixture of Fluxana powder (FX-X50-2, 50% Li-tetraborate and 50% Li-metaborate) in the sample:Fluxana with a ratio of 1:10. A few drops of LiBr were added to avoid gluing the melt onto the platinum vessel. The measurement was performed using X-ray fluorescence spectroscopy (Thermo Scientific ARL Perform'X Sequential XRF, 60 kV, 40 mA, Thermo electron SA, Ecublens, Switzerland) with OXAS software. The XRF data were characterised using the software UniQuant 5. The calculated analytical errors were <0.1% for Ca, <6% for Mg, Al and Si and <15% for Na and K.

The non-carbonate fraction of rocks and soil was determined arbitrary as the sum of Al_2O_3, SiO_2, Fe_2O_3, Na_2O and K_2O determined by the XRF.

A semiquantitative X-ray diffraction analysis was performed on dried pulverised samples in the range from 4° to 70° in steps of 0.013° under cleanroom conditions with an Empyrean PANalytical X-Ray Diffractometer (Thermo Scientific, Thermo electron SA, Ecublens, Switzerland). The mineral analysis along with standard-less Rietveld refinement was performed on XRD data using the X'Pert Highscore plus 4.1 software.

A stable isotope analysis of carbon and oxygen in carbonate was performed o using the Europa 20-20 isotope ratio mass spectrometer upgraded with a Sercon HS source assembly and 20-22 electronic suite (Sercon Ltd., Crewe, U.K.). The pulverised samples were placed in Labco Exetainers®, dried overnight at 60 °C, sealed with septum caps and flushed with He (6.0). Then, 0.3 mL of hot 100% H_3PO_4 was injected into the vials. The acid was prepared following the instructions by Sharp (2017). The samples were digested for 72 h at 40 °C in a thermoblock fitted to the ANCA TG preparation unit for the trace gas analysis. All samples were measured in triplicate, and the results were accepted if the standard deviation was equal or less than 0.1‰ for both $\delta^{13}C$ and $\delta^{18}O$. If the deviation was larger, the analysis was repeated until the required precision was achieved. The measurements were calibrated to the VPDB scale using NBS 19 and IAEA CO-9 certified reference materials. As controls, working standards IAEA-C2 with $\delta^{13}C_{VPDB}$ and $\delta^{18}O_{VPDB}$ values of −8.25 and −8.97‰, respectively (Bernasconi et al., 2018), and KH2 with $\delta^{13}C_{VPDB}$ and $\delta^{18}O_{VPDB}$ values of 1.89 and −2.90‰, respectively, were used.

Concentrations of Ca, Mg, U and U isotopes were analysed in bulk samples and in leachable fractions. A soft, less invasive leaching procedure was applied to extract carbonate-associated metals (Štrok and Smodiš, 2010); however, the procedure dissolved some easily soluble hydroxides and adsorbed metals in addition to calcite (Malov and Zykov, 2020). Therefore, it is hereafter referred to as a 'leachable' fraction, while the undissolved residue is referred to as a 'residual' fraction and was comprised of acid insoluble minerals (e.g. silicates, oxides). Theoretically, if dolomite were present in the sample, a minor portion of undissolved dolomite would also occur in the residual fraction (Rovan et al., 2020).

For leaching, an aliquot of 1 g of tufa powder was precisely weighed in a centrifuge tube. 15 mL of 1 M sodium acetate (NaAc) in 25% acetic acid (HAc) were added, and the samples were then shaken for 2 h at room temperature. Next, the samples were centrifuged and filtered through 0.45 μm pore size Millipore filters and washed two times with 5 mL of deionized water. Small aliquots of the eluate were used for Mg and Ca analyses by ICP-MS, while the remainder was dried on a hotplate and re-dissolved in 5 mL of 3 M HNO_3 to be prepared for column chromatography.

The concentrations of total carbon (C), organic carbon (OC) and nitrogen (N) were determined in 5 to 7 mg of dried sediment ground in an agate mortar before analysis. Aliquots for total carbon and nitrogen were prepared in tin containers, while samples for organic carbon were weighed in silver containers. Prior to analysis, the aliquots for OC were acid-treated with 1 M, 2 M and 6 M HCl. This procedure was repeated until no visual effervescence was evident. The analysis was performed using a Vario Micro Cube elemental analyser (Elementar Langenselbold, Germany) with a combustion at 1150 °C. The samples were analysed in replicates, and the results were reported as the mean and standard deviation per sample.

The total dissolution of the samples (Trdin et al., 2017) was performed to test the separation of detrital fraction in the leached samples. Aliquots of 1 g of powdered samples were digested with lithium borates fusion. In a platinum crucible, approximately 4 g of lithium borates were added to the sample, and the fusion was performed in a Claisse LeoNeo furnace at 1050 °C for 23 min. The obtained glass was dissolved in glass beakers at 135 °C in 100 mL of deionized water with the addition of 10 mL of concentrated HNO_3. After dissolution, the beakers were left on the hotplate with continuous stirring until the volume was reduced to 50 mL, which resulted in a 2–3 M HNO_3 solution. The solution was then cooled to 90 °C, and 1 mL of 0.2 M polyethylene glycol solution (PEG) was added to remove silicates. The stirring continued for 1 h. The precipitate was left to settle overnight, and the remaining solution was filtered and subjected to column chromatography.

U was separated from the matrix using UTEVA extraction chromatography in the same way as was described for the water samples.

The U concentration in the samples was determined using an Agilent 8800 Triple Quadrupole ICP-MS (Agilent Technologies, California, USA) following a measurement protocol that was described by Rovan and Štrok (2019). Interference correction and external calibration were performed using the U standard reference material SRM-3164 (National Institute of Standards & Technology, Gaithersburg, MD, USA).

3.2.3. U isotope measurements

U isotope ratios were measured using a Nu plasma II (Nu Instruments Ltd., UK) MC-ICP-MS with the high-efficiency Aridus II™ (Cetac

Technologies, NE, USA) sample desolvation system as described by Rovan and Štrok (2019). The total process blanks for the U isotopic analysis ranged from 0.08 ng to 0.28 ng. The procedural blanks were negligible compared to the amount of U contained in the samples. U isotope ratios are expressed as delta notation (Eq. (1)) and as $^{234}U/^{238}U$ activity ratios (Eq. (3)).

$$\frac{^{234}U}{^{238}U}\text{activity ratio} = \lambda_{234}/\lambda_{238} \times \left(^{234}U/^{238}U\right)_{corrected} \quad (3)$$

The $\delta^{238}U$ values were determined relative to the IRMM-184 standard and were recalculated to the $\delta^{238}U_{CRM\text{-}112a}$ values to assure comparability with previously published data (Standards for Nuclear Safety Security and Safeguards Unit, 2019). The $^{234}U/^{238}U$ activity ratio was calculated from the mass bias corrected isotope ratios and by using the decay constants (λ_{234} and λ_{238}) reported by Cheng et al. (2013).

The long-term analytical precision was assessed using the measurements of the U isotopic standard (IRMM-184) at a 5 ng mL^{-1} concentration over a period of 15 months. The mean values of the $^{235}U/^{238}U$ and $^{234}U/^{238}U$ isotope ratios of U standards are $(7.2622 \pm 0.0049) \times 10^{-3}$, $(5.314 \pm 0.017) \times 10^{-5}$ and $(3.113 \pm 0.083) \times 10^{-6}$, respectively. The measured values are in agreement with certified reference values (Standards for Nuclear Safety Security and Safeguards Unit, 2019). The uncertainty on measured U isotopes was expressed in terms of the expanded uncertainty ($k = 2$) and was assessed from different sources of measurement uncertainty, which are described in more detail by Rovan and Štrok (2019). The reproducibility of replicate measurements was within 0.5% for the $^{234}U/^{238}U$ isotope ratios and 0.1‰ for the $\delta^{238}U$ values.

4. Results and discussion

Tabulated results of the elemental and isotopic analyses of water, tufa, bedrock, and soil samples are available in Supplementary materials.

4.1. Precipitation of tufa: insight from C and O stable isotopes

The prerequisite for the precipitation of tufa is a high supersaturation of water with respect to calcite. While the carbonate sheath impregnations in sluggish water were reported already at 1.6 to 2 times supersaturation (Merz-Preiß and Riding, 1999), the spontaneous carbonate precipitation at cascades and waterfalls occurs when supersaturation increases up to 4 to <10 times (Srdoc et al., 1985; Herman and Lorah, 1988). The precipitation of carbonate in rivers is triggered by the degassing of CO_2, particularly (but not only) at topographic discontinuities (Pedley, 1990; Drysdale et al., 2002; Andrews and Brasier, 2005; Golubic et al., 2008; Capezzuoli et al., 2014). Major and trace elements, such as Mg, Sr, U etc., can co-precipitate with calcite, where the partitioning between water and carbonate results from the cumulative effects of the chemical composition of water, temperature, pH, speciation and adsorption on mineral surfaces, precipitation rate and microbial communities in the river (Rihs et al., 2000; Huang and Fairchild, 2001; Frank et al., 2006; Saunders et al., 2014; Chen et al., 2016; Ritter et al., 2018).

In the Krka River, a strong degassing of ^{13}C-depleted CO_2 without any notable $CaCO_3$ precipitation occurred between the spring (site K1) and Bilušića buk (K2), which is reflected by a decreased pCO_2 and concentration of DIC, an increased $\delta^{13}C$ value of DIC and an increased saturation index of calcite (Fig. 2a and b). In the tufa precipitating section of the river (sites K2–K6), the saturation index varied between 0.83 and 1.05, i.e. 6.8 to 11.1 times supersaturation. These values are very close to the SI_{calc} values reported for late summer in the period from 2001 to 2002 (0.87 to 1.17) (Lojen et al., 2004). The measured data on water in this study are only a snapshot of the physicochemical situation of the river, whereas the accumulation of tufa is a slow process, which proceeds at a rate of <1 to about 19 mm $year^{-1}$ (Maric et al., 2020). Individual hand samples of tufa analysed in this study were 5 to 10 cm thick, which means that their accumulation took several years to decades. Therefore, the isotopic composition of C and O in tufa shall be compared with the long-term ranges of historic data on the $\delta^{13}C$ values of DIC and the $\delta^{18}O$ values of water, which are presented in Fig. 2c and d (ranges of values taken from Lojen et al., 2004; Lojen et al., 2009; Cukrov et al., 2012). The $\delta^{13}C$ values of recent tufa were on average -9.60 ± 0.65‰ and within the range of a ±1‰ deviation from the $\delta^{13}C$ values of DIC as predicted by Romanek et al. (1992) and Jimenez-Lopez et al. (2006). Although at the lowermost waterfall both analysed samples were strongly depleted in ^{13}C compared to the DIC analysed in this study, the $\delta^{13}C$ values of both tufa samples were within the long-term range of the $\delta^{13}C$ values of DIC. The O isotope composition of recent tufa analysed in this study were on average -8.08 ± 0.41‰ and was almost identical to those determined 20 years earlier at the same locations (Lojen et al., 2004). The differences among the pairs of tufa samples from opposite riverbanks at sites K5 and K6 found in this study are surprisingly large because the differences in the $\delta^{18}O$ values of water measured at both riverbanks were small or within the analytical uncertainty.

Bonacci et al. (2017) analysed the hydrological situation at site K6 (Skradinski buk) in detail. The entire waterfall area consists of several unevenly distributed steps and dozens of small basins, where water flows relatively independently on the left and the right side during low flow conditions. The tributary Čikola that discharges into the Krka River from the left (eastern) side just above the waterfall regularly dries out during the summer, but the subsurface groundwater discharge continues through numerous submerged springs downstream into the estuary (Liu et al., 2019). Considering this, it is obvious that the hydrological conditions, hydrochemical composition and isotopic characteristics at the right and the left side of the river can be different. Unfortunately, no hydrological study of the analysed cascades of Roški slap area (K5) was done, but similar to Skradinski buk, the surface river flow splits into several channels and pools separated by small tufa islands with abundant vegetation at a lower discharge. Meanwhile, at a high water level, both riverbanks are flooded. On one hand, this can explain the larger fraction of detrital non-carbonate matter in tufa at site K5 compared to site K6 (5.3 and 6.3% at K5a and b compared to 1.5 and 1.7% at K6a and b) and the higher amount of organic carbon in tufa (0.6 and 1.1 wt% at K5a and b compared to 0.53% at both K6 sites, Table S2, Supplementary materials). The 2019 sampling campaign was conducted at a high water level when the left and right flows of the river were connected. At a low discharge, the differences could be larger, but no long-term monitoring data of $\delta^{18}O$ values of water at both river banks are available.

The carbonate precipitation in isotopic disequilibrium in rivers is not uncommon (Yan et al., 2020) and was observed even in controlled laboratory experiments for both C (Jimenez-Lopez et al., 2006) and O isotopes (Dietzel et al., 2009). Previous studies showed that in the Krka River, the carbonate precipitated close to the O isotope equilibrium only at the uppermost tufa barrier (K2). Further downstream, the discrepancy between the equilibrium $\delta^{18}O$ values of water and precipitate formed in the actual temperature range increased with an increasing annual average temperature and an increasing annual temperature variability of river water. In contrast to C isotopes, the O isotope fractionation between water and carbonate during the precipitation of calcite depends on the precipitation rate to a similar or even greater extent as on the temperature (Dietzel et al., 2009). The calculated calcite precipitation rates for the given conditions of temperature, pH and chemical composition of water at the time of sampling varied from $4.9 \cdot 10^{-9}$ g cm^{-2} s^{-1} at sites K2 and K6b to $5.6 \cdot 10^{-9}$ g cm^{-2} s^{-1} at site K4 (Table 1). Dietzel et al. (2009) found that with an increasing precipitation rate, the O isotope fractionation between water and calcite decreases, and this was confirmed by the study of tufa precipitation in a karstic river in Slovenia (Zavadlav et al., 2017). In the Krka River, the

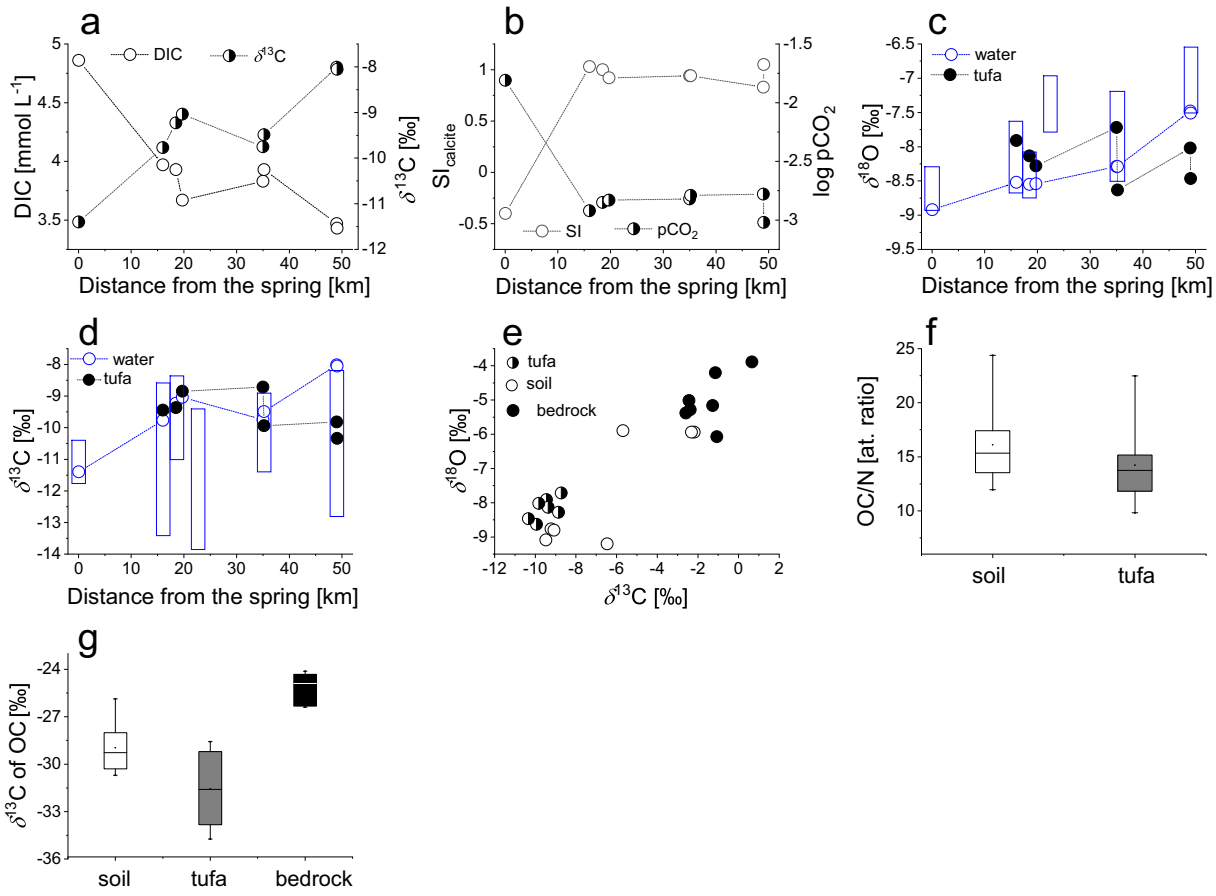

Fig. 2. Downstream variation of concentration and C stable isotope composition of dissolved inorganic carbon (a); saturation index of calcite and log pCO_2 (b); stable isotope composition of oxygen in the Krka River water and in tufa (c); stable isotope composition of dissolved inorganic C and carbonate in tufa (d); $\delta^{18}O$ vs. $\delta^{13}C$ plot of carbonate in tufa, soil and bedrock (e); ranges of values of organic C to total N ratios in soil and tufa (f); and ranges of $\delta^{13}C$ values of organic C in soil, tufa and bedrock (g). Hollow bars in (c, d) represent the range of values measured in the period 2000 to 2007 (Lojen et al., 2004; Lojen et al., 2009; Cukrov et al., 2012). The bar at 22 km represents the sampling site from 2001 to 2007 (Miljacka hydroelectric power plant), which was not accessible in 2019.

smallest O isotope fractionation between water and tufa was indeed observed at sites with the highest precipitation rates (K4, K5b), while a larger O isotope fractionation was found at sites with lower precipitation rates (K2 and K6). Still, the differences in the precipitation rate cannot account for the big differences observed between O isotope composition of carbonate from both riverbanks at sites K5 and K6.

The $\delta^{13}C$ and $\delta^{18}O$ values of tufa can be affected by the incorporation of suspended detrital carbonate washed out from soil, bedrock and eroded recent or old tufa. Fig. 2e shows the $\delta^{13}C$ vs. $\delta^{18}O$ plot of bedrock, soil and tufa, and it is evident that tufa and bedrock carbonates form two separate groups, while the soil samples plot was in between the two groups with the whole range of values from typical of marine carbonate to typical of tufa. The lowest measured $\delta^{18}O$ value in the soil (−9.48‰) was even lower than in any of the tufa samples. The presence of detrital carbonate from bedrock and soil can thus considerably alter the C and O isotope signatures of tufa and can be captured in tufa along with non-carbonate detritus. Hence, the relatively high $\delta^{13}C$ values of tufa at sites K5a and K6a could be attributed to the washout of ^{13}C-

Table 1
Measured physicochemical, elemental parameters, and isotopic analyses in river water from Krka River (K) and Zrmanja River (Z). Exact locations of sampling sites can be found in Fig. 1.

Site	Distance from the spring [km]	Temperature [°C]	pH	Conductivity [μS cm^{-2}]	Redox potential [mV]	Total alkalinity [mmol L^{-1}]	Particulate matter [mg L^{-1}]	Ca^{2+} [mg L^{-1}]	Mg^{2+} [mg L^{-1}]	R · 10^{-9} [g cm^{-2} s^{-1}]
K1	0	9.9	7.11	426	111	4.03	4.2	56.8	14.3	ND
K2	16	15.0	8.21	726	96	4.01	2.0	119.7	19.7	4.9
K3	18.8	16.7	8.15	686	94	3.95	0.3	116.5	20.0	5.3
K4	19.7	17.2	8.10	688	98	3.68	<0.1	117.3	20.6	5.6
K5a	35	19.6	8.12	612	138	3.85	<0.1	104.1	17.1	5.4
K5b	35.5	19.7	8.10	617	111	3.94	1.6	105.3	17.3	5.5
K6a	49	23.1	8.07	481	163	3.48	6.5	83.7	12.8	5.2
K6b	49.5	23.6	8.31	469	113	3.54	13.5	80.8	12.0	4.9
Z1	16	NM	NM	NM	NM	3.41	1.3	52.6	11.0	ND
Z2	38	NM	NM	NM	NM	4.30	<0.1	70.7	6.2	ND
Z3	50	NM	NM	NM	NM	3.74	0.3	64.9	6.1	ND

NM: not measured; ND: not determined.

enriched soil and bedrock carbonate. This assumption is also supported by the C/N ratio of sedimentary organic matter in tufa (Fig. 2f), which is 14.6 ± 4.3 and is similar to that of the soil (16.1 ± 3.7). The same range of values was reported for riverine particulate organic matter, where fine particulates had an OC/N ratio between 10 and 16 and coarse ones between 14 and 25 (Hatten et al., 2012). C/N ratios above 20 are typical of terrestrial organic matter derived from vascular plants (Meyers, 1994), while the microbial (algal and bacterial) biomass has C/N ratios typically <10 (Kendall et al., 2001). The low $\delta^{13}C$ values of sedimentary organic C in tufa (average value of −31.57 ± 2.32‰, Fig. 2g) reflect a mixture of soil organic matter and autochthonous riverine organic material derived from algae and highly ^{13}C-depleted vascular plants growing in the spray zone of the river (Marcenko et al., 1989).

The variability of the C and O isotopic signatures of Krka River tufa at consecutive barriers is therefore interpreted as a result of an annual fluctuation of the isotope composition of water, DIC, temperature, variable precipitation rates and variable fractions of lithic and soil carbonate incorporated into the tufa fabrics.

4.2. Uranium in water

The total dissolved U concentrations in the Krka and Zrmanja water fell within the typical range for rivers fed from carbonate aquifers (Alshamsi et al., 2013; Guerrero et al., 2016; Chen et al., 2020; Rovan et al., 2020). In the tufa-precipitating river, the concentration of dissolved U decreased toward the estuary from 0.67 to 0.46 ng L^{-1} (Fig. 3a). A similar trend with maximum concentrations of dissolved load between sites K2 and K4 (16 to 20 km downstream from the spring) and decreasing values afterwards was observed for other metals in this (Table 1) and previous studies (Cukrov et al., 2008, 2013), which indicates that U, along with other dissolved metals, is subjected to active self-purification processes of adsorption, sedimentation and co-precipitation with carbonate. The main sedimentation basins are lakes Brljan between sites K2 and K3, the lake between sites K4 and K5 and lake Visovac between sites K5 and K6 with average sedimentation rates of 10, 8 and 7 mm per year, respectively (Cukrov et al., 2013). The Zrmanja River was depleted in U compared to the Krka River (Table S1, Supplementary materials), and the invasion of water masses from the Zrmanja sub-catchment between sites K3 and K5 could also contribute to the decrease in the dissolved U load in the Krka River. A conspicuous difference in the dissolved U concentration in the areas of cascades at sites K5 (Roški slap) and K6 (Skradinski buk) occurred between the right (K5a, K6a) and the left riverbanks (K5b, K6b). This difference is also reflected in the U content in bulk and leachable fraction of tufa at sites K5a and K5b; however, no such difference was noted in tufa at sites K6a and K6b (Fig. 3a). Because tufa integrates a long-term hydrochemical composition of water, it can be expected that at sites K5a and b, the difference in the U concentration in the water at both riverbanks is likely systematic. Different environmental conditions at both riverbanks can obviously affect the dissolved U concentrations in the river at very short distances, which are then transferred to the river sediments.

The dissolved $^{234}U/^{238}U$ activity ratio has become a trusted tracer of groundwater and river water sources, reflecting the variability of the discharge and lithology of the catchment (Fleischer, 1982; Riotte and Chabaux, 1999; Chabaux et al., 2003; Riotte et al., 2003; Durand et al., 2005; Chabaux et al., 2008; Kraemer and Brabets, 2012; Guerrero et al., 2016; Zebracki et al., 2017; Navarro-Martínez et al., 2020; Rovan et al., 2020). The enrichment of water in ^{234}U relative to bedrock depends on the rock type, permeability and groundwater transit time as well as on the weathering rate (Li et al., 2018). The interpretation of $^{234}U/^{238}U$ activity ratios in water is therefore never simple or straightforward.

The activity ratios of $^{234}U/^{238}U$ in the Krka River (Fig. 3b) generally decreased downstream from the spring, from 1.49 to 1.28, and is consistent with the findings of Suksi et al. (2006). In the reducing environment of the aquifer, due to the alpha recoil effect, ^{234}U is oxidised, while ^{238}U remains in the less soluble reduced form. Consequently, the solubility of ^{234}U is increased, and the $^{234}U/^{238}U$ activity ratio in groundwater at the orifice exceeds the equilibrium value of 1. In the aerated stream, the dissolution of U-containing particulates continues in the oxygenated environment, where ^{234}U and ^{238}U are released to the solution in equal proportions. Therefore, the $^{234}U/^{238}U$ activity ratio slowly decreases downstream. Another process that could decrease the dissolved $^{234}U/^{238}U$ activity ratio downstream is the dissolution of the finest suspended mineral particles. Thollon et al. (2020) analysed the river sediments of world largest rivers and found that the sediments in rivers draining catchment areas composed of sedimentary rocks generally had a clay fraction (that is transported as suspended load) enriched in ^{238}U compared to the coarser fraction. The dissolution of the finest suspended particles with a $^{234}U/^{238}U$ activity ratio around or below 1 would in fact push the $^{234}U/^{238}U$ activity ratio of water toward lower values.

The plateau of $^{234}U/^{238}U$ activity ratios of 1.38–1.39 occurred between sites K3 and K5, while at the lowermost waterfall, the $^{234}U/^{238}U$ activity dropped to 1.29. The Zrmanja River at site Z1 upstream from the temporary sink had a $^{234}U/^{238}U$ activity ratio of 1.51, so the inflow of ^{234}U-enriched groundwater from the Zrmanja River in the K3-K5 river sections could in part neutralise the general decreasing trend of the $^{234}U/^{238}U$ activity ratio of Krka River water. However, since the annual variability of the $^{234}U/^{238}U$ activity ratio of Zrmanja River water and the travel time of groundwater discharging into the Krka river are not known, the influence of Zrmanja River water on the $^{234}U/^{238}U$ activity ratios of Krka river at this stage remains a plausible explanation but cannot be quantified.

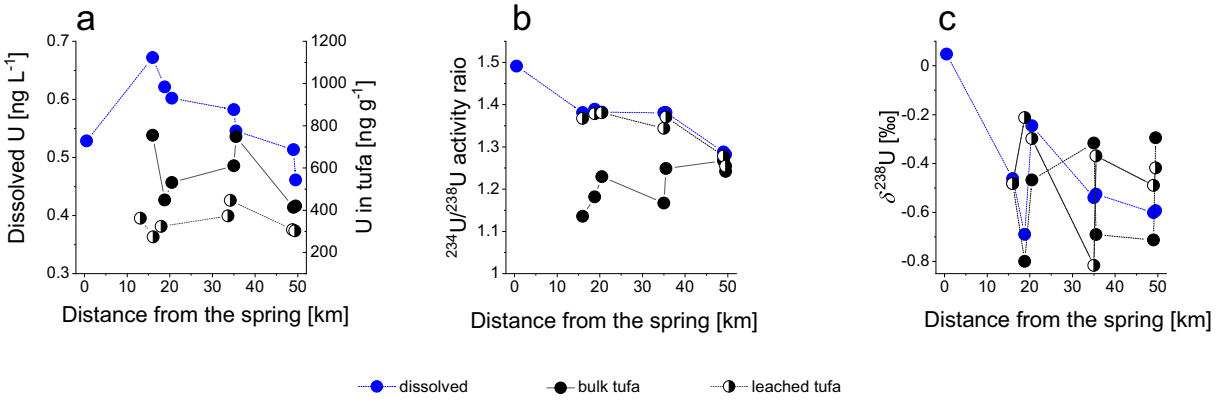

Fig. 3. Downstream variations of U concentrations (a); $^{234}U/^{238}U$ activity ratios (b); and $\delta^{238}U$ values (c) in dissolved U in water, bulk tufa and in the leachable fraction of tufa.

The flow section between sites K2-K5 is characterised by massive tufa precipitation at waterfalls and by intensive sedimentation in lentic sections of the river. Sedimentation of fine particles in lakes between sites K2 and K3, K4 and K5 and K5 and K6 is reflected by the decreased amount of particulate matter in the river between sites K2 and K5, from 2.0 mg L^{-1} to <0.1 mg L^{-1} (Table 1). Brennecka et al. (2011) and Jemison et al. (2016) analysed the ^{235}U-^{238}U isotope fractionation induced by the adsorption of U species onto mineral surfaces and found that adsorption on common sedimentary minerals, such as quartz, illite, goethite or Mn oxides, produces a notable fractionation with adsorbed U(VI) enriched in a light (^{235}U) isotope. Assuming the same mechanism could operate in the ^{234}U-^{238}U isotope pair as well and that at pH values around 8 in oxygenated water the dissolved U is present in U(VI) ionic complexes with carbonate, preferential adsorption on mineral particles followed by the sedimentation of lighter U(VI) would then push the $^{234}U/^{238}U$ activity ratio of water toward lower values. The same explanation applies to the Zrmanja River, which is also intersected with several barriers with lentic sections in-between.

The downstream behaviour of the $\delta^{238}U$ values of the Zrmanja River is similar to that of the $^{234}U/^{238}U$ activity ratios (a decrease with the distance from the spring, −0.02‰ to −0.60‰), while in the Krka River, a conspicuous anomaly occurs in the short river section K2-K4, where values first decreased from −0.46‰ to −0.69‰ and then increased to −0.25‰ (Fig. 3c).

In both rivers, a positive correlation between the $\delta^{238}U$ and $^{234}U/^{238}U$ activity ratios existed, although in the Zrmanja River, the correlation was rather weak ($r^2 = 0.89$ in Krka and 0.53 in Zrmanja). Apparently, this should be a contradiction, but all $\delta^{238}U$ values of river water were in the range of those of contributing bedrock and soil (Fig. 4d). The dissolved U could thus be derived from the weathering of leachable and residual fractions of any of them in different and seasonally changing and/or event-driven proportions. In particular, the residual U in bedrock had a large range of $\delta^{238}U$ values (−1.78 to +1.53‰). It was established that the $\delta^{238}U$ values of dissolved U in rivers resemble those of bedrock and that $\delta^{238}U$ values of river water largely reflect the U isotope variations between catchments, with no correlation to the $^{234}U/^{238}U$ activity ratios or hydrochemical parameters (Weyer et al., 2008; Andersen et al., 2016; Noordmann et al., 2016). While the analysed bedrock and soils show a rather narrow range of $\delta^{238}U$ values for bulk samples, the U isotope composition of leachable and in particular the residual U fraction were much more variable (for leachable fraction −0.78 to −0.11‰ for bedrock, −0.56 to −0.03‰ for soil; residual −1.78 to +1.53‰ in bedrock, −0.56 to −0.03‰ in soil). Therefore, the variability of the $\delta^{238}U$ values of dissolved U in rivers could be to a greater extent governed by the isotopically more diverse residual U fractions of the bedrock and soil.

4.3. Uranium in tufa

The C and O isotope analyses of tufa in the Krka–Zrmanja aquifer showed that the bedrock and soil contributed not only non-carbonate detritus and organic matter, but also detrital carbonate that altered the isotopic composition of carbonate. It is therefore reasonable to assume, that the concentrations and isotope composition of U in carbonate fraction of tufa would be affected by the soil- and bedrock-derived carbonate, too.

The only previous data on U concentration in tufa from the Krka River (Franciškovic-Bilinski et al., 2004) was in the same range of values as in this study (Fig. 4a). Frank et al. (2006) analysed a drill core from a post-glacial tufa sequence in Thuringia (Germany), found that U concentrations and isotopic compositions varied according to accumulation rate and texture, and were more likely to reflect the changes of the U concentration and isotope composition of precipitating water than contamination with non-carbonate detritus. The tufa from the Krka and Zrmanja Rivers was formed in different sedimentary environments (cascades at sites K2, K4 and K6, paludal settings at K5 and Z3 and dam at K3). The bulk U concentrations showed no relation with the depositional setting, while the leachable (predominantly carbonate) U concentration was higher at paludal sites, while cascade and dam tufa were in approximately the same range of values.

The majority of U in recent tufa was bound to a leachable fraction (60–75%), which is less than in bedrock (70–88%) but much more than in the soil (14–33%) (Fig. 4a, Table S3, Supplementary materials). The exceptions were sites K2 (cascade) and Z3 (Zrmanja River, paludal tufa), where only 48% and 38% of U, respectively were leachable. Obviously, the governing factor for the incorporation of U into the leachable fraction of tufa is the concentration of dissolved U, which co-precipitates with the carbonate phase or is adsorbed to detrital minerals and

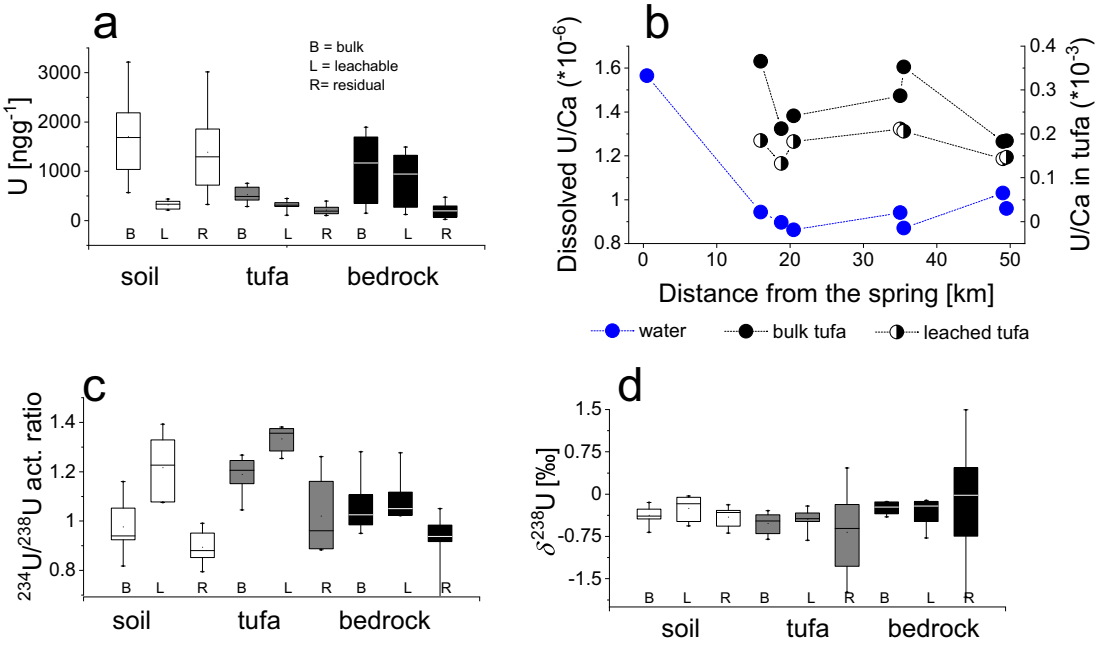

Fig. 4. Ranges of U concentrations in bulk, leachable and residual fractions of soil, tufa and bedrock (a); downstream variation of U/Ca ratio in water, bulk and the leachable fraction of tufa (b); ranges of $^{234}U/^{238}U$ activity ratios (c); and $\delta^{238}U$ values (d) in bulk, leachable and residual fractions of soil, tufa and bedrock.

deposited in tufa. The high affinity of $U(VI)O_2^{2+}$ to carbonate in an aerated environment results in the formation of $UO_2(CO_3)_2^{2-}$ complexes at pH < 6 and $UO_2(CO_3)_3^{4-}$ at a pH > 8. On one hand, this increases the solubility of U (for instance from soil) (Elless and Lee, 1998), while on the other hand, it facilitates the adsorption of U to carbonate surfaces (Krestou and Panias, 2004; Kelly et al., 2006) and its co-precipitation with calcite (Cumberland et al., 2016; Chen et al., 2016).

The composite processes of adsorption and co-precipitation of U in carbonate were suggested by Rihs et al. (2000), who found irregular U concentrations in a downstream profile of carbonate precipitated from a CO_2-rich geothermal spring, where the apparent partitioning coefficients of U decreased with advanced precipitation. In the Krka River, the U/Ca ratio of water (Fig. 4b) decreased from sites K2 to K4 and then slightly increased toward K6. The $(U/Ca)_{carb}$ ratio of tufa scattered irregularly downstream, yielding downstream scattering of apparent distribution coefficients of U ($K_U = (U:Ca)_{carbonate} / (U:Ca)_{water}$) between 0.14 and 0.24 (0.06 in the Zrmanja River). These values are lower than those calculated by Rihs et al. (2000) for thermal water but close to values reported by Meece and Benninger (1993) for coral carbonate (0.05 to <0.2). No correlation between K_U and temperature, pH or precipitation rate was observed. Obviously, the U partitioning between water and leachable fraction of tufa in the Krka River is affected by several processes, which cannot be unambiguously disentangled and are further complicated by the diffuse groundwater recharge and consecutive interchange of the lentic and lotic sections of the river flow, which most likely plays a significant role in the U geochemistry.

The $^{234}U/^{238}U$ ratio of the leachable fraction in recent tufa resembles the $^{234}U/^{238}U$ activity ratio of water (1.25–1.37 in tufa and 1.28–1.49 in water) (Fig. 3b). No information on ^{234}U-^{238}U isotope fractionation during the precipitation of carbonate could be found in the literature. The obtained differences are small but larger than the uncertainty of the measurement at all sites except K4 and can be attributed to the presence of soil- and bedrock derived detrital carbonate in tufa (Fig. 4c).

In contrast to $^{234}U/^{238}U$, the $^{238}U/^{235}U$ isotope fractionation during the precipitation of carbonate from aquatic solutions was studied in many laboratory experiments. At the pH range typical of karst water (7.5 and 8.5), no resolvable $^{238}U/^{235}U$ isotope fractionation could be observed (Chen et al., 2016), implying that the carbonate $\delta^{238}U$ value should be the same as that of the mother solution. Further experiments with seawater showed that the $^{238}U/^{235}U$ isotope fractionation could depend on the pH, ionic strength, pCO_2 and Mg^{2+} and Ca^{2+} concentrations (Chen et al., 2017). In natural terrestrial environments, highly variable U isotope fractionation was observed in speleothems, i.e. in authigenic carbonates precipitated in stable cave conditions from drip water (Stirling et al., 2007), while for river carbonate no data could be found. The $\delta^{238}U$ values of the leachable fraction of recent tufa analysed in this study were between −0.82 and −0.21‰. The $\delta^{238}U$ values of the residual U fraction in tufa varied between −1.73 and +0.46‰ compared to −1.78 to +1.53‰ in the residual fraction of bedrock and −0.69 to −0.19‰ in the soil (Fig. 4d). Clearly, the residual fraction of tufa is a mixture of bedrock- and soil-derived detritus. The isotope separation between leachable U and river water was between −0.28 and +0.48‰ (Fig. 3c), although it is assumed that authigenic carbonates incorporate $\delta^{238}U$ values of the mother solution without significant isotope fractionation (Stirling et al., 2007; Andersen et al., 2014; Chen et al., 2016). For sample sites K2, K4, K5b and K6, this was indeed the case (most were within the standard uncertainty of the analysis of ~0.1‰). Small differences can be explained by the isotope fractionation during adsorption on mineral surfaces, which was found to be around 0.2‰ (Brennecka et al., 2011; Jemison et al., 2016). Similar isotope fractionation was reported to occur during the abiotic reductive precipitation of U (Brown et al., 2018), although this would be less likely in aerated river environment. At sites K3 and K5a, the differences in the $\delta^{238}U$ values between the leachable fraction of tufa and river water were too large to be attributed to adsorption-related fractionation. In the tufa from site K3, the leachable $\delta^{238}U$ values are 0.48‰ higher than the $\delta^{238}U$ values of the water, while at site K5a, the leachable fraction of tufa is depleted in ^{238}U compared to the river water or any other leachable U source. Similar to $^{234}U/^{238}U$, a long-term observation of the isotopic composition of dissolved U and particulate U in water would be necessary to shed more light on U isotope fractionation in the tufa-precipitating stream.

4.3.1. Can U isotopes be the identifier of authigenic carbonate in tufa?

To roughly estimate the possible contributions of detrital leachable U from soil and bedrock to leachable U in tufa, the IsoSource mixing model (EPA) was used to calculate the mixing ratios of several contributing sources; however, the uncertainty of the results is highly dependent on the uncertainties of the end-members, which are in the case of tufa in the Krka River large. For calculation, the average $^{234}U/^{238}U$ activity ratios of soil and bedrock leachable fractions (1.22 and 1.08, respectively) and the $^{234}U/^{238}U$ activity ratio of water at each site were used (Figs. 3b and 4c). The calculation revealed that in the upper reaches of the Krka River (sites K2–K4), the most feasible combinations of sources were 80–84% of authigenic carbonate, 11–13% of soil carbonate and 5–7% of bedrock carbonate. In lower reaches, at cascades K6a and K6b, the distribution of sources was 41–61% of carbonate, 30–38% of soil and 9–13% of bedrock detrital carbonate. For paludal sites K5a,b and Z3, the most feasible distribution was 65–81% of authigenic carbonate, 13–26% of soil and 6–9% of bedrock detrital carbonate. The uncertainty for soil and bedrock contributions in some cases exceeded 100% because the $^{234}U/^{238}U$ activity ratios of soil and bedrock carbonate are highly variable. Interestingly, both potential sources had $^{234}U/^{238}U$ activity ratios higher than 1. The enrichment of soils in ^{234}U was explained by the addition of U to soils from ^{234}U-enriched soil solutions (Huckle et al., 2016), while the high $^{234}U/^{238}U$ activity ratio of the leachable fraction of bedrock was surprising because all analysed rock formations were of the Cretaceous to the Eocene age (Mamudžic, 1971); however, a bulk $^{234}U/^{238}U$ activity ratio up to 1.05 was previously reported by Deschamps et al. (2004) for limestone along stylolitic discontinuities in Mesozoic limestone. Although the mechanisms of the migration of ^{234}U were not fully explained, the same processes could alter the $^{234}U/^{238}U$ activity ratio of tectonically strongly disturbed carbonate rocks at Dinaric carbonate formations. The calculation for the estimation of contributing sources based on $\delta^{238}U$ values was not only speculative but, in some cases, not even possible because the tufa had lower or higher $\delta^{238}U$ values of leachable U than any of the potential contributing parameters. The best conclusion at this stage would be that the authigenic carbonate precipitated from a U-bearing river mostly resembles the $^{234}U/^{238}U$ activity ratio of dissolved U in water, but the presence of a detrital U-containing leachable phase can result in deviations from the $^{234}U/^{238}U$ activity ratio of dissolved U.

5. Conclusions

This study has demonstrated the use of U and its isotope ratios to better understand different possible environmental influences on tufa formation and to evaluate the contribution of the authigenic and detrital carbonate in tufa samples from the Krka and Zrmanja Rivers in Croatia, which could potentially be used to estimate the CO_2 storage in river carbonate. In the studied samples, the variability of classical geochemical parameters and traditional isotopes ($\delta^{18}O$, $\delta^{13}C$) showed that both detrital and authigenic carbonates are present in tufa and are affected by the suspended detrital carbonate in the river washed out from the bedrock and soil. The downstream profile of U concentration and the activity ratios of $^{234}U/^{238}U$ in the Krka River water showed effects of active self-purification processes of sedimentation, co-precipitation with carbonate, and adsorption of U species onto mineral surfaces followed by the preferential sedimentation of ^{234}U. The large scattering of $\delta^{238}U$ values in the Krka River showed that $\delta^{238}U$ is a much more sensitive tracer of bedrock composition than the $^{234}U/^{238}U$ activity ratios. The governing factor of the incorporation of U into tufa is the concentration

of dissolved U, which accumulates in the carbonate precipitate; however, the U partitioning between water and carbonate can be also affected by complicated hydrology, variable temperature, hydrological situation, and by detrital carbonates.

Overall, the U distribution and isotope composition in the carbonate fraction of tufa are controlled by many mechanisms and cannot be solely explained by any of them. In such a complex karst aquifer, geochemical parameters, traditional isotopes and U isotopic compositions are affected by the sources of materials for tufa precipitation and by environmental processes. Based on the present data and knowledge, some of the explanations are still speculative, so a long-term seasonal and event-based observation of the entire system, including water, suspended materials and precipitates, is needed to confirm the universality of conclusions.

CRediT authorship contribution statement

Leja Rovan: Conceptualization, Data curation, Methodology, Visualization, Writing – original draft. **Tea Zuliani:** Methodology, Writing – review & editing. **Barbara Horvat:** Methodology, Writing – review & editing. **Tjaša Kanduč:** Methodology, Writing – review & editing. **Polona Vreča:** Methodology, Writing – review & editing. **Qasim Jamil:** Methodology. **Branko Čermelj:** Methodology, Writing – review & editing. **Elvira Bura-Nakić:** Funding acquisition, Data curation, Writing – review & editing. **Neven Cukrov:** Writing – review & editing. **Marko Štrok:** Supervision, Writing – review & editing. **Sonja Lojen:** Conceptualization, Data curation, Funding acquisition, Project administration, Visualization, Writing – original draft.

Declaration of competing interest

The authors declare that they have no known competing financial interests or personal relationships that could have appeared to influence the work reported in this paper.

Acknowledgement

This study was supported by the Slovenian Research Agency through the research project J1-9179, research programmes P1-0143 and P2-0075, the Young Researcher's programme and the Slovenian-Croatian bilateral collaboration project BI-HR-20-21-039. Research within this work was partially also funded by the Croatian Science Foundation, project IP-2018-01-7813, "REDOX". Special thanks to Mr. Tomislav Bulat (R. Bošković Institute), Mr. Stojan Žigon and Ms. Klara Nagode (J. Stefan Institute) for technical assistance and the National Park 'Krka' for the permission for sampling.

Appendix A. Supplementary data

Supplementary data to this article can be found online at https://doi.org/10.1016/j.scitotenv.2021.149103.

References

Alshamsi, D.M., Murad, A.A., Aldahan, A., Hou, X., 2013. Uranium isotopes in carbonate aquifers of arid region setting. J. Radioanal. Nucl. Chem. 298, 1899–1905.

Andersen, M.B., Romaniello, S., Vance, D., Little, S.H., Herdman, R., Lyons, T.W., 2014. A modern framework for the interpretation of 238U/235U in studies of ancient ocean redox. Earth Planet. Sci. Lett. 400, 184–194.

Andersen, M.B., Stirling, C.H., Weyer, S., 2017. Uranium isotope fractionation. Rev. Mineral. Geochem. 82, 799–850.

Andersen, M.B., Stirling, C.H., Zimmermann, B., Halliday, A.N., 2010. Precise determination of the open ocean 234U/238U composition. Geochem. Geophys. Geosyst. 11. https://doi.org/10.1029/2010GC003318.

Andersen, M.B., Vance, D., Morford, J.L., Bura-Nakic, E., Breitenbach, S.F.M., Och, L., 2016. Closing in on the marine 238U/235U budget. Chem. Geol. 420, 11–22.

Andrews, J.E., Brasier, A.T., 2005. Seasonal records of climatic change in annually laminated tufas: short review and future prospects. J. Quat. Sci. 20, 411–421.

Avak, H., Brand, W.A., 1995. The finning MAT HDO-equilibration - a fully automated H2O/gas phase equilibration system for hydrogen and oxygen isotope analyses. Thermo Electron. Corp. Appl. News 11, 1–13.

Banks, V.J., Jones, P.F., 2012. Hydrogeological significance of secondary terrestrial carbonate deposition in karst environments. In: Kazemi, G.A. (Ed.), Hydrogeology - A Global Perspective. Intech, pp. 43–78.

Bernasconi, S.M., Müller, I.A., Bergmann, K.D., Breitenbach, S.F.M., Fernandez, A., Hodell, D.A., Jaggi, M., Meckler, A.N., Millan, I., Ziegler, M., 2018. Reducing uncertainties in carbonate clumped isotope analysis through consistent carbonate-based standardization. Geochem. Geophys. Geosyst. 19, 2895–2914.

Bonacci, O., 1999. Water circulation in karst and determination of catchment areas: example of the river zrmanja. Hydrol. Sci. J. 44, 373–386.

Bonacci, O., Andric, I., Roje-Bonacci, T., 2017. Hydrological analysis of skradinski Buk tufa waterfall (Krka River, dinaric karst, Croatia). Environ. Earth Sci. 76, 669.

Bonacci, O., Jukic, D., Ljubenkov, I., 2006. Definition of catchment area in karst: case of the rivers Krcic and Krka, Croatia. Hydrol. Sci. J. 51, 682–699.

Bourdon, B., Bureau, S., Andersen, M.B., Pili, E., Hubert, A., 2009. Weathering rates from top to bottom in a carbonate environment. Chem. Geol. 258, 275–287.

Brennecka, G.A., Wasylenki, L.E., Bargar, J.R., Weyer, S., Anbar, A.D., 2011. Uranium isotope fractionation during adsorption to mn-oxyhydroxides. Environ. Sci. Technol. 45, 1370–1375.

Brasier, A.T., Andrews, J.E., Marca-Bell, A.D., Dennis, P.F., 2010. Depositional continuity of seasonally laminated tufas: implications for d18O based palaeotemperatures. Glob. Planet. Chang. 71, 160–167.

Brown, S.T., Basu, A., Ding, X., Christensen, J.N., DePaolo, D.J., 2018. Uranium isotope fractionation by abiotic reductive precipitation. Proc. Natl. Acad. Sci. 115, 8688–8693.

Buhmann, D., Dreybrodt, W., 1985. The kinetics of calcite dissolution and precipitation in geologically relevant situations of karst areas: 1. Open system. Chem. Geol. 48, 189–211.

Capezzuoli, E., Gandin, A., Pedley, M., 2014. Decoding tufa and travertine (fresh water carbonates) in the sedimentary record: the state of the art. Sedimentology 61, 1–21.

Carter, J.F., Barwick, V.J., 2011. Good practice guide for isotope ratio mass spectrometry. FIRMS 1–41.

Chabaux, F., Bourdon, B., Riotte, J., 2008. Chapter 3 U-series geochemistry in weathering profiles, river waters and lakes. Radioact. Environ. 13, 49–104.

Chabaux, F., Riotte, J., Dequincey, O., 2003. U-th-ra fractionation during weathering and river transport. Rev. Mineral. Geochem. 52, 533–576.

Chen, Q., Liu, S., He, H., Tang, J., Zhao, J., Feng, Y., Yang, X., Zhou, H., 2020. Seasonal variations of uranium in karst waters from northeastern Sichuan, Central China and controlling mechanisms. Geochem. Int. 58, 103–112.

Chen, X., Romaniello, S.J., Anbar, A.D., 2017. Uranium isotope fractionation induced by aqueous speciation: implications for U isotopes in marine CaCO3 as a paleoredox proxy. Geochim. Cosmochim. Acta 215, 162–172.

Chen, X., Romaniello, S.J., Herrmann, A.D., Wasylenki, L.E., Anbar, A.D., 2016. Uranium isotope fractionation during coprecipitation with aragonite and calcite. Geochim. Cosmochim. Acta 188, 189–207.

Cheng, H., Lawrence Edwards, R., Shen, C.-C., Polyak, V.J., Asmerom, Y., Woodhead, J., Hellstrom, J., Wang, Y., Kong, X., Spötl, C., Wang, X., Calvin Alexander, E., 2013. Improvements in 230Th dating, 230Th and 234U half-life values, and U–Th isotopic measurements by multi-collector inductively coupled plasma mass spectrometry. Earth Planet. Sci. Lett. 371–372, 82–91.

Cukrov, N., Cmuk, P., Mlakar, M., Omanovic, D., 2008. Spatial distribution of trace metals in the Krka River, Croatia: an example of the self-purification. Chemosphere 72, 1559–1566.

Cukrov, N., Cuculic, V., Barišic, D., Lojen, S., Mikelic, I.L., Orešcanin, V., Vdovic, N., Fiket, Ž., Cermelj, B., Mlakar, M., 2013. Elemental and isotopic records in recent fluvio-lacustrine sediments in karstic river Krka, Croatia. J. Geochem. Explor. 134, 51–60.

Cukrov, N., Tepic, N., Omanovic, D., Lojen, S., Bura-Nakic, E., Vojvodic, V., Pižeta, I., 2012. Qualitative interpretation of physico-chemical and isotopic parameters in the Krka River (Croatia) assessed by multivariate statistical analysis. Int. J. Environ. Anal. Chem. 92, 1187–1199.

Cumberland, S.A., Douglas, G., Grice, K., Moreau, J.W., 2016. Uranium mobility in organic matter-rich sediments: a review of geological and geochemical processes. Earth Sci. Rev. 159, 160–185.

De Boever, E., Brasier, A.T., Foubert, A., Kele, S., 2017. What do we really know about early diagenesis of non-marine carbonates? Sediment. Geol. 361, 25–51.

Dedic, Ž., Ilijanic, N., Miko, S., 2018. A mineralogical and petrographic study of evaporites from Mali kukor, Vranjkovici and Slane stine deposits (Upper permian, Dalmatia, Croatia). Geol. Croat. 71, 19–28.

Deschamps, P., Hillaire-Marcel, C., Michelot, J.-L., Doucelance, R., Ghaleb, B., Buschaert, S., 2004. 234U/238U disequilibrium along stylolitic discontinuities in deep mesozoic limestone formations of the eastern Paris basin: evidence for discrete uranium mobility over the last 1–2 million years. Hydrol. Earth Syst. Sci. 8, 35–46.

Dietzel, M., Tang, J., Leis, A., Köhler, S.J., 2009. Oxygen isotopic fractionation during inorganic calcite precipitation - effects of temperature, precipitation rate and pH. Chem. Geol. 268, 107–115.

Drysdale, R.N., Taylor, M.P., Ihlenfeld, C., 2002. Factors controlling the chemical evolution of travertine-depositing rivers of the barkly karst, northern Australia. Hydrol. Process. 16, 2941–2962.

Durand, S., Chabaux, F., Rihs, S., Duringer, P., Elsass, P., 2005. U isotope ratios as tracers of groundwater inputs into surface waters: example of the upper Rhine hydrosystem. Chem. Geol. 220, 1–19.

Elless, M.P., Lee, S.Y., 1998. Uranium solubility of carbonate-rich uranium-contaminated soils. Water Air Soil Pollut. 107, 147–162.

EPA - United States Environmental Protection Agency, n... IsoSource: Stable Isotope Mixing Model for Partitioning an Excess Number of Sources, Version 1.3.1. accessible

at. https://www.epa.gov/eco-research/stable-isotope-mixing-models-estimating-source-proportions.
Epstein, S., Mayeda, T., 1953. Variation of O18 content of waters from natural sources. Geochim. Cosmochim. Acta 4, 213–224.
Fleischer, R.L., 1982. Alpha-recoil damage and solution effects in minerals: uranium isotopic disequilibrium and radon release. Geochim. Cosmochim. Acta 46, 2191–2201.
Ford, T.D., Pedley, H.M., 1996. A review of tufa and travertine deposits of the world. Earth Sci. Rev. 41, 117–175.
Franciškovic-Bilinski, S., Barišic, D., Vertacnik, A., Bilinski, H., Prohic, E., 2004. Characterization of tufa from the dinaric karst of Croatia: mineralogy, geochemistry and discussion of climate conditions. Facies 50, 183–193.
Frank, N., Kober, B., Mangini, A., 2006. Carbonate precipitation, U-series dating and U-isotopic variations in a holocene travertine platform at Bad Langensalza - Thuringia Basin, Germany. Quaternaire 17, 333–342.
Gat, J.R., Gonfiantini, R., 1981. Stable Isotope Hydrology: Deuterium and Oxygen-18 in the Water Cycle. IAEA, Vienna, Austria.
Gieskes, J.M., 1974. The alkalinity-total carbon dioxide system in seawater. In: Goldberg, E.D. (Ed.), Marine Chemistry of the Sea. John Wiley and Sons, New York, pp. 123–151.
Golubic, S., Violante, C., Plenkovic-Moraj, A., Gragasovic, T., 2008. Travertines and calcareous tufa deposits: an insight into diagenesis. Geol. Croat. 61, 363–378.
González Martín, J.A., González Amuchastegui, M.J., 2014. Las Tobas en España. SEG, Badajoz.
Guerrero, J.L., Vallejos, Á., Cerón, J.C., Sánchez-Martos, F., Pulido-Bosch, A., Bolívar, J.P., 2016. U-isotopes and 226Ra as tracers of hydrogeochemical processes in carbonated karst aquifers from arid areas. J. Environ. Radioact. 158–159, 9–20.
Hatten, J.A., Goñi, M.A., Wheatcroft, R.A., 2012. Chemical characteristics of particulate organic matter from a small, mountainous river system in the Oregon coast range, USA. Biogeochemistry 107, 43–66.
Herman, J.S., Lorah, M.M., 1988. Calcite precipitation rates in the field: measurement and prediction for a travertine-depositing stream. Geochim. Cosmochim. Acta 52, 2347–2355.
Huang, Y., Fairchild, I.J., 2001. Partitioning of Sr2 and Mg2 into calcite under karst-analogue experimental conditions. Geochim. Cosmochim. Acta 65, 47–62.
Huckle, D., Ma, L., McIntosh, J., Vázquez-Ortega, A., Rasmussen, C., Chorover, J., 2016. U-series isotopic signatures of soils and headwater streams in a semi-arid complex volcanic terrain. Chem. Geol. 445, 68–83.
Jemison, N.E., Johnson, T.M., Shiel, A.E., Lundstrom, C.C., 2016. Uranium isotopic fractionation induced by U(VI) adsorption onto common aquifer minerals. Environ. Sci. Technol. 50, 12232–12240.
Jimenez-Lopez, C., Romanek, C.S., Caballero, E., 2006. Carbon isotope fractionation in synthetic magnesian calcite. Geochim. Cosmochim. Acta 70, 1163–1171.
Kelly, S.D., Rasbury, E.T., Chattopadhyay, S., Kropf, A.J., Kemner, K.M., 2006. Evidence of a stable uranyl site in ancient organic-rich calcite. Environ. Sci. Technol. 40, 2262–2268.
Kendall, C., Silva, S.R., Kelly, V.J., 2001. Carbon and nitrogen isotopic compositions of particulate organic matter in four large river systems across the United States. Hydrol. Process. 15, 1301–1346.
Kraemer, T.F., Brabets, T.P., 2012. Uranium isotopes (234U/238U) in rivers of the Yukon Basin (Alaska and Canada) as an aid in identifying water sources, with implications for monitoring hydrologic change in arctic regions. Hydrogeol. J. 20, 469–481.
Krestou, A., Panias, D., 2004. Uranium (VI) speciation diagrams in the UO22/CO32-/H2O system at 25oC. Eur. J. Miner. Process. Environ. Prot. 4, 113–129.
Kulušic, A., Borojevic Šostaric, S., 2014. Dinaride evaporite mélange: diagenesis of the Kosovo Polje evaporites. Geol. Croat. 67, 59–74.
Leng, M.J., Lamb, A.L., Heaton, T.H.E., Marshall, J.D., Wolfe, B.B., Jones, M.D., Holmes, J.A., Arrowsmith, C., 2006. Isotopes in lake sediments. In: Leng, M.J. (Ed.), Isotopes in Paleoenvironmental Research. Springer, Dordrecht, pp. 147–184.
Li, L., Chen, J., Chen, T., Chen, Y., Hedding, D.W., Li, G., Li, L., Li, T., Robinson, L.F., West, A.J., Wu, W., You, C.-F., Zhao, L., Li, G., 2018. Weathering dynamics reflected by the response of riverine uranium isotope disequilibrium to changes in denudation rate. Earth Planet. Sci. Lett. 500, 136–144.
Liu, J., Hrustic, E., Du, J., Gašparovic, B., Cankovic, M., Cukrov, N., Zhu, Z., Zhang, R., 2019. Net submarine groundwater-derived dissolved inorganic nutrients and carbon input to the oligotrophic stratified karstic estuary of the Krka River (Adriatic Sea, Croatia). J. Geophys. Res. Ocean. 124, 4334–4349.
Liu, Z., Dreybrod, W., 1997. Dissolution kinetics of calcium carbonate minerals in H2O-CO2 solutions in turbulent flow: the role of the diffusion boundary layer and the slow reaction H2O + CO2 ↔ H+ + HCO3−. Geochim. Cosmochim. Acta 61, 2879–2889.
Liu, Z., Svensson, U., Dreybrodt, W., Daoxian, Y., Buhmann, D., 1995. Hydrodynamic control of inorganic calcite precipitation in huanglong ravine, China: field measurements and theoretical prediction of deposition rates. Geochim. Cosmochim. Acta 59, 3087–3097.
Lojen, S., Dolenec, T., Vokal, B., Cukrov, N., Mihelcic, G., Papesch, W., 2004. C and O stable isotope variability in recent freshwater carbonates (River krka, Croatia). Sedimentology 51, 361–375.
Lojen, S., Trkov, A., Ščancar, J., Vázquez-Navarro, J.A., Cukrov, N., 2009. Continuous 60-year stable isotopic and earth-alkali element records in a modern laminated tufa (Jaruga, river krka, Croatia): implications for climate reconstruction. Chem. Geol. 258, 242–250.
Malov, A.I., Zykov, S.B., 2020. Study of the mobilization of uranium isotopes in a sandstone aquifer in combination with groundwater data. Water 12, 112.
Mamudžic, P., 1971. Osnovna geološka karta SFRJ 1: 100 000, list Šibenik (Basic Geological Map of SFT Yugoslavia, page Šibenik). Geological Survey of Yugoslavia, Belgrade.
Marcenko, E., Srdoc, D., Golubic, S., Pezdic, J., Head, M.J., 1989. Carbon uptake in aquatic plants deduced from their natural 13C and 14C content. Radiocarbon 31, 785–794.
Maric, I., Šiljeg, A., Cukrov, N., Roland, V., Domazetovic, F., 2020. How fast does tufa grow? Very high-resolution measurement of the tufa growth rate on artificial substrates by the development of a contactless image-based modelling device. Earth Surf. Process. Landf. 45, 2331–2349.
Meece, D.E., Benninger, L.K., 1993. The coprecipitation of pu and other radionuclides with CaCO3. Geochim. Cosmochim. Acta 57, 1447–1458.
Merz-Preiß, M., Riding, R., 1999. Cyanobacterial tufa calcification in two freshwater streams: ambient environment, chemical thresholds and biological processes. Sediment. Geol. 126, 103–124.
Meyers, P.A., 1994. Preservation of elemental and isotopic source identification of sedimentary organic matter. Chem. Geol. 114, 289–302.
Miyajima, T., Miyajima, Y., Hanba, Y.T., Yoshii, K., Koitabashi, T., Wada, E., 1995. Determining the stable isotope ratio of total dissolved inorganic carbon in lake water by GC/C/IIRMS. Limnol. Oceanogr. 40, 994–1000.
Navarro-Martínez, F., Sánchez-Martos, F., Salas, García A., Gisbert, Gallego J., 2020. The use of major, trace elements and uranium isotopic ratio (234U/238U) for tracing of hydrogeochemical evolution of surface waters in the Andarax River catchment (SE Spain). J. Geochem. Explor. 213, 106533.
Noordmann, J., Weyer, S., Georg, R.B., Jöns, S., Sharma, M., 2016. 238U/235U isotope ratios of crustal material, rivers and products of hydrothermal alteration: new insights on the oceanic U isotope mass balance. Isot. Environ. Health Stud. 52, 141–163.
Nyachoti, S., Jin, L., Tweedie, C.E., Ma, L., 2019. Insight into factors controlling formation rates of pedogenic carbonates: a combined geochemical and isotopic approach in dryland soils of the US southwest. Chem. Geol. 527, 118503.
Parkhurst, D.L., Appelo, C.A.J., 1999. User's Guide to PHREEQC (Version 2) – A Computer 25 Program for Speciation, Batch-reaction, One-dimensional Transport, and Inverse Geochemical Calculations (Denver, Colorado).
Pedley, M., 1990. Classification and environmental models of cool freshwater tufas. Sediment. Geol. 68, 143–154.
Pedley, M., 2009. Tufas and travertines of the Mediterranean region: a testing ground for freshwater carbonate concepts and developments. Sedimentology 56, 221–246.
Rihs, S., Condomines, M., Sigmarsson, O., 2000. U, Ra and Ba incorporation during precipitation of hydrothermal carbonates: implications for 226Ra-Ba dating of impure travertines. Geochim. Cosmochim. Acta 64, 661–671.
Riotte, J., Chabaux, F., 1999. (234U/238U) activity ratios in freshwaters as tracers of hydrological processes: the strengbach watershed (Vosges, France). Geochim. Cosmochim. Acta 63, 1263–1275.
Riotte, J., Chabaux, F., Benedetti, M., Dia, A., Gérard, M., Boulègue, J., Etamé, J., 2003. Uranium colloidal transport and origin of the 234U–238U fractionation in surface waters: new insights from Mount Cameroon. Chem. Geol. 202, 365–381.
Ritter, S.M., Isenbeck-Schröter, M., Schröder-Ritzrau, A., Scholz, C., Rheinberger, S., Höfle, B., Frank, N., 2018. Trace element partitioning in fluvial tufa reveals variable portions of biologically influenced calcite precipitation. Geochim. Cosmochim. Acta 225, 176–191.
Rogerson, M., Pedley, H.M., Wadhawan, J.D., Middleton, R., 2008. New insights into biological influence on the geochemistry of freshwater carbonate deposits. Geochim. Cosmochim. Acta 72, 4976–4987.
Romanek, C.S., Grossman, E.L., Morse, J.W., 1992. Carbon isotopic fractionation in synthetic aragonite and calcite: effects of temperature and precipitation rate. Geochim. Cosmochim. Acta 56, 419–430.
Rovan, L., Lojen, S., Zuliani, T., Kanduc, T., Petric, M., Horvat, B., Rusjan, S., Štrok, M., 2020. Comparison of uranium isotopes and classical geochemical tracers in karst aquifer of Ljubljanica River catchment (Slovenia). Water 12, 2064.
Rovan, L., Štrok, M., 2019. Optimization of the sample preparation and measurement protocol for the analysis of uranium isotopes by MC-ICP-MS without spike addition. J. Anal. At. Spectrom. 34, 1882–1891.
Saunders, P., Rogerson, M., Wadhawan, J.D., Greenway, G., Pedley, H.M., 2014. Mg/Ca ratios in freshwater microbial carbonates: thermodynamic, kinetic and vital effects. Geochim. Cosmochim. Acta 147, 107–118.
Sharp, Z., 2017. Principles of Stable Isotope Geochemistry. 2nd edition. Pearson Education.
Spötl, C., 2005. A robust and fast method of sampling and analysis of d13C of dissolved inorganic carbon in ground waters. Isot. Environ. Health Stud. 41, 217–221.
Srdoc, D., Horvatincic, N., Obelic, B., Krajcar, I., Sliepcevic, A., 1985. Procesi taloženja kalcita u krškim vodama s posebnim osvrtom na Plitvicka jezera (Calcite deposition processes in karstwaters with special emphasis on the Plitvice Lakes, Yugoslavia). KRS Jugosl. 11, 1–104.
Standards for Nuclear Safety Security and Safeguards Unit, 2019. Nuclear Certified Reference Materials 2019. Geel, Belgium.
Stirling, C.H., Andersen, M.B., Potter, E.-K., Halliday, A.N., 2007. Low-temperature isotopic fractionation of uranium. Earth Planet. Sci. Lett. 264, 208–225.
Suksi, J., Rasilainen, K., Pitkänen, P., 2006. Variations in 234U/238U activity ratios in groundwater—a key to flow system characterisation? Phys. Chem. Earth, Parts A/B/C 31, 556–571.
Štrok, M., Smodiš, B., 2010. Fractionation of natural radionuclides in soils from the vicinity of a former uranium mine Žirovski vrh, Slovenia. J. Environ. Radioact. 101, 22–28.
Tanweer, A., Gröning, M., Van Duren, M., Jaklitsch, M., Pöltenstein, L., 2009. TEL Technical Note No. 43 Stable Isotope Internal Laboratory Water Standards: Preparation, Calibration and Storage. International Atomic Energy Agency, Vienna.
Teichert, B.M.A., Eisenhauer, A., Bohrmann, G., Haase-Schramm, A., Bock, B., Linke, P., 2003. U/Th systematics and ages of authigenic carbonates from hydrate ridge, Cascadia margin: recorders of fluid flow variations. Geochim. Cosmochim. Acta 67, 3845–3857.
Thollon, M., Bayon, G., Toucanne, S., Trinquier, A., Germain, Y., Dosseto, A., 2020. The distribution of (234U/238U) activity ratios in river sediments. Geochim. Cosmochim. Acta 290, 216–234.

Trdin, M., Necemer, M., Benedik, L., 2017. Fast decomposition procedure of solid samples by lithium borates fusion employing salicylic acid. Anal. Chem. 89, 3169–3176.

Wang, R.-M., You, C.-F., 2013. Precise determination of U isotopic compositions in low concentration carbonate samples by MC-ICP-MS. Talanta 107, 67–73.

Weyer, S., Anbar, A.D., Gerdes, A., Gordon, G.W., Algeo, T.J., Boyle, E.A., 2008. Natural fractionation of 238U/235U. Geochim. Cosmochim. Acta 72, 345–359.

Yan, H., Liu, Z., Sun, H., 2020. Large degrees of carbon isotope disequilibrium during precipitation-associated degassing of CO2 in a mountain stream. Geochim. Cosmochim. Acta 273, 244–256.

Zavadlav, S., Rožic, B., Dolenec, M., Lojen, S., 2017. Stable isotopic and elemental characteristics of recent tufa from a karstic Krka River (south-East Slovenia): useful environmental proxies? Sedimentology 64, 808–831.

Zebracki, M., Cagnat, X., Gairoard, S., Cariou, N., Eyrolle-Boyer, F., Boulet, B., Antonelli, C., 2017. U isotopes distribution in the lower Rhone River and its implication on radionuclides disequilibrium within the decay series. J. Environ. Radioact. 178–179, 279–289.

Zhao, M.Y., Zheng, Y.F., Zhao, Y.Y., 2016. Seeking a geochemical identifier for authigenic carbonate. Nat. Commun. 7, 10885.